

Measurements of radiative B meson decays at Belle

Hanjin Kim* (on behalf of the Belle collaboration)

Yonsei University

E-mail: hanjin.kim@yonsei.ac.kr

The radiative B meson decays $\bar{B} \rightarrow X_s \gamma$, and $X_d \gamma$ provide good probes to new physics as new unknown particles can enter in the loop and change the branching fractions and the associated CP asymmetries. We present the analyses of radiative B decays for branching fractions and the direct CP asymmetries. In particular, we report the inclusive CP asymmetry of the $b \rightarrow s\gamma/d\gamma$ decays, recently obtained with the semi-inclusive and the lepton tagging method by the *Belle* collaboration. HQE parameters in shape-function scheme is obtained using the measured spectrum as well. We also present the results of the exclusive $\mathcal{B}(B^0 \rightarrow \phi\gamma)$, $\mathcal{B}(B_s^0 \rightarrow \phi\gamma)$, and $\mathcal{B}(B_s^0 \rightarrow \gamma\gamma)$.

*38th International Conference on High Energy Physics
3-10 August 2016
Chicago, USA*

*Speaker.

1. Introduction

The quark-level $b \rightarrow s\gamma$ decays have been studied since the discovery of $B \rightarrow K^*\gamma$ [1]. In the standard model (SM), such decays occur mainly through flavor-changing neutral current (FCNC) process which is depicted in the Fig. 1. The virtual W in the diagram may be replaced by a non-SM charged particle from new physics, e.g. charged higgs in supersymmetry (SUSY) models, which can affect the relevant branching fractions in comparison to those obtained from SM. Within the SM, these decays may appear via tree-level processes such as $b \rightarrow u\bar{u}s\gamma$ but its contributions is limited to less than 0.4% [2].

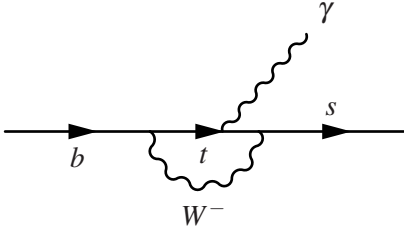


Figure 1: FCNC process of $b \rightarrow s\gamma$ decay

In the SM, the branching fraction of $b \rightarrow s\gamma$ has been calculated to Next-to-Next-to-Leading-Order (NNLO) correction [4]. The most recent branching fraction obtained from NNLO is, for the signal photon energy, E_γ^B , threshold, $E_\gamma^B > 1.6$ GeV, $\mathcal{B}(\bar{B} \rightarrow X_s\gamma)_{\text{NNLO}} = (3.36 \pm 0.23) \times 10^{-4}$ where the error is theoretical. The average of the experimentally measured values of the branching fraction $\mathcal{B}(\bar{B} \rightarrow X_s\gamma)_{\text{exp}} = (3.49 \pm 0.19) \times 10^{-4}$ [5, 6], where the error is combined for statistical, systematic, and shape-function systematics, with the same $E_\gamma^B > 1.6$ GeV threshold, show approximately 1σ deviation from this calculation. This consistency has provided severe constraints on new physics beyond the SM.

In addition to the branching fraction, the direct CP asymmetry of $b \rightarrow s\gamma$ decays can provide independent tests on new physics models and can be used to put constraints on models such as SUSY. The CP asymmetry is defined as follows :

$$A_{CP}(b \rightarrow s\gamma) = \frac{\Gamma(b \rightarrow s\gamma) - \Gamma(\bar{b} \rightarrow \bar{s}\gamma)}{\Gamma(b \rightarrow s\gamma) + \Gamma(\bar{b} \rightarrow \bar{s}\gamma)}$$

The current PDG value for the CP asymmetry of inclusive $b \rightarrow s\gamma$ decays is $A_{CP}(b \rightarrow s\gamma)_{\text{PDG}} = 0.015 \pm 0.020$.

2. Data Analysis

2.1 Experimental facility and the data set

We use data collected with the Belle detector[7] at the KEKB e^+e^- collider[8]. Integrated luminosities of the data amount 711 fb^{-1} , and 121 fb^{-1} collected at $\Upsilon(4S)$ and $\Upsilon(5S)$ resonances, respectively. The selection criteria is optimized and the $\bar{B} \rightarrow X_s\gamma$ signal efficiency is determined using a Monte Carlo (MC) simulation based on EvtGen[9] and GEANT3[10] to get the interaction kinematics and detector response simulated, respectively.

The inclusive spectrums of the $\bar{B} \rightarrow X_s\gamma$ signal events for E_γ^B and $M(X_s)$ are shaped with three models in the market; the Kagan-Neubert (KN) model[11], kinetic scheme[12], and the shape-function (SF)[13] scheme. All these models take two Heavy Quark Expansion (HQE) parameters, m_b and μ_π^2 as their shape parameters.

2.2 Semi-inclusive Method

With the semi-inclusive method, we reconstruct a signal B candidate by combining a high energy photon and a X_s which is reconstructed via one of the 38 X_s final states. The X_s final states employed in this study cover about 70% of the full-inclusive branching fraction of $\bar{B} \rightarrow X_s \gamma$. The photon candidate is required to have an energy in the center-of-mass (CM) frame between 1.8 and 3.4 GeV. Photon backgrounds arise from π^0 and η decays are rejected based on the invariant mass of two-photon system where the photon candidate is paired with another photon detected. The X_s reconstruction is also optimized by requiring the quality of charged tracks such as K^+ and π^+ and that of reconstructed neutral particles such as π^0 , η , and K_s^0 .

The yield of signal events are extracted from the maximum likelihood fitting on the beam-energy-constrained mass, $M_{bc} = \sqrt{(E_{beam}/c^2)^2 - |\vec{p}_B/c|^2}$, where E_{beam} is the beam energy and \vec{p}_B is a energy-momentum 4-vector obtained from the B candidate. In M_{bc} distribution, events with a well-reconstructed B candidate yield a peaking shape around the mass of B meson. The fitting procedure is implemented for 19 $M(X_s)$ bins spanning $0.6 < M(X_s) < 2.8$ GeV. The continuum events are efficiently suppressed by a neural network (NN) trained with topological variables. And based on the NN score, we select the best B candidate among the candidates reconstructed concurrently for a given event. D meson veto is also applied since D meson decays, especially $B \rightarrow D^{(*)} \rho^+$ is found peaking in M_{bc} distribution.

Systematic uncertainties arise from the missing modes (1.59%), $N_{B\bar{B}}$ (1.37%), the detector response (2.98%), selection criterion (3.38%), M_{bc} PDF modeling (5.06%), and the hadronization model (6.66%). The hadronization model uncertainty is associated with the fragmentation parameters of the EvtGen which decide the hadron fragmentation in the MC sample.

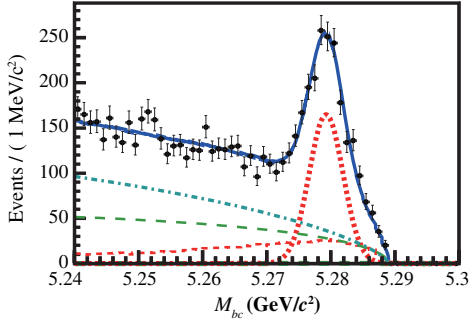


Figure 2: M_{bc} fit result for the bin $1.4 < M(X_s) < 1.5$ GeV/ c^2 . The plot shows the data (black points), the fit function (blue solid), the fit component of signal (red thick dashed), cross-feed (red thin dashed), non peaking $B\bar{B}$ background (green dashed), and $q\bar{q}$ background (blue dot-dashed).

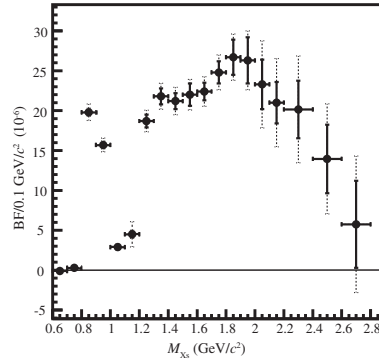


Figure 3: Partial branching fraction as a function of $M(X_s)$. The error bars correspond to the statistical (solid) and the quadratic sum of the statistical and systematic (dashed).

The partial branching fractions are obtained for each $M(X_s)$ bin with the signal yield and efficiency. Here the signal efficiencies are estimated by using the signal MC sample which is

shaped with the Kagan-Neubert model. The figure 3 shows the partial branching fraction results for the $M(X_s)$ range of interest. We report the total branching fraction for $M(X_s) < 2.8 \text{ GeV}/c^2$, $\mathcal{B}(\bar{B} \rightarrow X_s \gamma) = (3.51 \pm 0.17 \pm 0.33) \times 10^{-4}$ where the first uncertainty is statistical and the second is systematic. The E_γ^B threshold for this result is $E_\gamma^B > 1.9 \text{ GeV}$ [14].

2.3 Full-inclusive with Lepton Tagging Method

For a full-inclusive study, we employ the lepton tagging method. The lepton tagging method requires a high energy lepton emerging from leptonic decays of a recoil B meson. The requirement on a high energy lepton effectively reduces the $q\bar{q}$ background. And with the charge of the lepton given, we are able to obtain the direct CP asymmetry. On the signal B meson's side, we require a high energy (signal) photon leaving the final state of X_{s+d} unknown to access the full decay width through the CM energy of the signal photon spectrum, E_γ^* .

As requirements are mostly related to the high energy photon, lots of backgrounds arise in the signal E_γ^* region. Especially there are significant contributions from π^0 and η decays. We manage to suppress a large part of background events using a Boosted Decision Tree (BDT), but the background events still remain dominant especially in a low signal E_γ^* region. The continuum events remaining are subtracted by using a scaled off-resonance sample, which may limit the statistical precision of measurements.

For a measurement of the branching fraction, it is essential to estimate the background yields as precisely as possible. To achieve MC/DATA agreement for the background events, we calibrate the MC events. The background events from π^0 and η decays with large control samples, and the other backgrounds such as bremsstrahlung, mis-identified hadrons, etc. are separately calibrated and/or assigned with a conservative systematic uncertainties on their yields.

The raw CP asymmetry of $\bar{B} \rightarrow X_{s+d} \gamma$ is measured with $A_{CP}^{\text{meas}} = [(N^+ - N^-)/(N^+ + N^-)]$, where $N^{+(-)}$ is the total number of positively (negatively) lepton-tagged events remaining after subtracting all the background events for a given photon energy threshold. We correct the raw asymmetry due to possible asymmetries in the $B\bar{B}$ background subtracted, $A_{\text{bkg}} \approx (0.0 \pm 0.7)\%$, possible asymmetries in the detection of leptons, $A_{\text{det}} \approx (0.0 \pm 0.3)\%$, and probability of a wrong charge-flavor correlation, $\omega \approx 14\%$. The corrected CP asymmetry is defined as $A_{CP} = (1 - 2\omega)^{-1}(A_{CP}^{\text{meas}} - A_{\text{bkg}} - A_{\text{det}})$.

Since the systematic uncertainties correlated between B and anti- B are canceled out by definition of A_{CP}^{meas} . The dominant systematic uncertainty arises from correcting the raw asymmetry. We present $A_{CP}(\bar{B} \rightarrow X_{s+d} \gamma) = (2.2 \pm 3.9_{\text{stat}} \pm 0.9_{\text{sys}})\%$ for the threshold $E_\gamma^* > 2.1 \text{ GeV}$ [15].

The branching fraction of the $\bar{B} \rightarrow X_{s+d} \gamma$ is obtained using the E_γ^* spectrum obtained after subtracting the calibrated background spectrum (figure 4). We unfold the spectrum using the Singular Value Composition (SVD) method to remove the resolution effect of the detector. And the signal efficiencies are estimated by averaging values from three signal models; the KN model, kinetic scheme, and the SF scheme. The E_γ^* threshold is fixed at 1.8 GeV so that we can obtain the best result considering the extrapolation. Finally the $\mathcal{B}(B \rightarrow X_d \gamma)$ is excluded from $\mathcal{B}(B \rightarrow X_{s+d} \gamma)$ using $|V_{td}/V_{ts}|^2 \approx 4\%$.

The systematic uncertainty arises from the background yields (5.2%), the number of $B\bar{B}$ pairs (1.4%), the continuum background subtraction (1.3%), and the possible BDT mis-modeling in the $B\bar{B}$ MC (1.4%). We report the inclusive branching fraction, $\mathcal{B}(\bar{B} \rightarrow X_s \gamma) = (3.01 \pm 0.10_{\text{stat}} \pm$

$0.19_{\text{syst}} \pm 0.08_{\text{model}} \times 10^{-4}$ with the threshold $E_\gamma^* > 1.8$ GeV[16]. It is mentionable that the precision of this single measurement almost reaches the precision level of the current HFAG/PDG average.

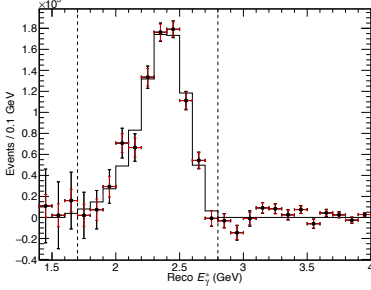


Figure 4: E_γ^* spectrum before unfolding. The error bars correspond to the statistical (red) and the quadratic sum of the statistical and systematic (black). The black solid line is the best fit of the theoretical spectrum.

In addition to the branching fraction measurement, we utilize the E_γ^* spectrum (Figure 4) to estimate the HQE parameters. The traditional way of obtaining the parameters in SF scheme is translating the parameters in the kinetic scheme measured from $B \rightarrow X_u l^+ \nu_l$ decay. However, it is reported that the spectrum of $\bar{B} \rightarrow X_s \gamma$ can also be used to determine the HQE parameters and finally can result in the V_{ub} [13]. The parameters are estimated by fitting the measured spectrum with the theoretical spectrum. We fit the measured spectrum with the theoretical spectrum expected by the shape-function (SF) scheme to minimize the χ^2 between two spectrums. The full experimental covariance matrix of the background-subtracted spectrum is used for the fitting procedure. The theoretical spectrum is folded with a response matrix representing the EM calorimeter resolution effect, and the Doppler smearing of the transform between the B rest frame and the CM frame. We find the HQE parameters in the SF scheme, $m_b(SF) = 4.626 \pm 0.028$ GeV/ c^2 and $\mu_\pi^2(SF) = 0.301 \pm 0.063$ GeV/ c^2 with a correlation, $\rho = -0.701$, where the errors are quadratic sums of the statistical and systematic errors[16].

Considering the current HFAG average for the HQE parameters[5] there are two interesting interpretation can be made on our results. First, the our precision is as good as the averages. Fitting the $\bar{B} \rightarrow X_s \gamma$ spectrum directly can produce a good measurement for the extraction of V_{ub} compared to the traditional method. Second, the difference in values is not negligible, especially for $\mu_\pi^2(SF)$. This much of difference may result in lowering V_{ub} by about 6% (3%) for the endpoint analysis with $E_{\text{lepton}} > 2.0$ GeV (1.0 GeV).

3. Exclusive modes

We also measure the branching fraction of the exclusive decay modes. For the $B^0 \rightarrow \phi \gamma$ decay, we report a limit for the branching fraction, $\mathcal{B}(B^0 \rightarrow \phi \gamma) < 1.0 \times 10^{-7}$ at 90% C.L where the SM prediction corresponds to $\mathcal{O}(10^{-11 \sim -12})$ [17]. For the exclusive $b \rightarrow s \gamma$ and $b \rightarrow s \gamma \gamma$ decays, we report $\mathcal{B}(B_s^0 \rightarrow \phi \gamma) = (3.6 \pm 0.5_{\text{stat}} \pm 0.3_{\text{syst}} \pm 0.6(f_s)) \times 10^{-5}$ and $\mathcal{B}(B_s^0 \rightarrow \gamma \gamma) < (3.1) \times 10^{-6}$ at 90% C.L, respectively where f_s is the fraction of $B_s^{(*)} \bar{B}_s^{(*)}$ in $b\bar{b}$ events[18].

4. Conclusion

As of Nov. 2016, the *Belle* collaboration present the most precise measurements for the branching fraction and the direct CP asymmetry of $\bar{B} \rightarrow X_s \gamma$ decay. We also determine the HQE parameters in SF scheme with fitting the $\bar{B} \rightarrow X_s \gamma$ spectrum directly. And this kind of approach for the

extraction of HQE parameter may be competitive to the traditional method using the $B \rightarrow X_u l^+ \nu_l$ decay. The most stringent limits are also determined for $B^0 \rightarrow \phi \gamma$ and $B_s^0 \rightarrow \gamma \gamma$ by the Belle collaboration.

References

- [1] R. Ammar *et al.* [CLEO Collaboration], *Evidence for penguin-diagram decays: First observation of $B \rightarrow K^*(892)\gamma$* , *Phys. Rev. Lett.* **71** (1993) 674.
- [2] Maciej Kaminski, Mikolaj Misiak, Michal Poradzinski, *Tree-level contributions to $B \rightarrow X_s \gamma$* , *Physic. Rev.* **D86** 094004, [hep-ph/1209.0965].
- [3] A.J. Buras, A. Czarnecki, M. Misiak and J. Urban, *Completing the NLO QCD calculation of $\bar{B} \rightarrow X_s \gamma$* , *Nucl. Phys. B* **631** 219, [hep-ph/0203135].
- [4] M. Misiak *et al.*, *Updated NNLO QCD predictions for the weak radiative B-meson decays*, *Phys. Rev. Lett.* **114** 221801, [arXiv:1503.01789].
- [5] Y. Amhis *et al.* [Heavy Flavor Averaging Group], *Averages of b-hadron, c-hadron, and τ -lepton properties as of summer 2014*, [hep-ex/1412.7515] and online update at <http://www.slac.stanford.edu/xorg/hfag>.
- [6] K. A. Olive *et al.* [Particle Data Group Collaboration], *Chin. Phys. C* **38**, 090001 (2014) and 2015 update. doi:10.1088/1674-1137/38/9/090001
- [7] A. Abashian *et al.* [Belle Collaboration], *Nucl. Instrum. Methods Phys. Res. Sec. A* **479** 117; also see detector section in J. Brodzicka *et al.*, *Prog. Theor. Exp. Phys.* **2012** 04D001.
- [8] S. Kurokawa and E. Kikutani, *Nucl. Instrum. Methods Phys. Res. Sect. A* **499** 1, and other papers included in this Volume; T. Abe *et al.*, *Prog. Theor. Exp. Phys.* **2013** 03A001 and following articles up to 03A011.
- [9] D.J. Lange, *Nucl. Instrum. Meth.* **A462** (2001) 152-155, doi: 10.1016/S0168-9002(01)00089-4
- [10] R. Brun *et al.*, GEANT 3.21, Cern/DD/ee/84-1 (1986).
- [11] A. L. Kagan and M. Neubert, *ACD Anatomy of $B \rightarrow X_s \gamma$ Decays* *Eur. Phys. J. C* **7** (1999) 5 [hep-ph/9805303]
- [12] B. Benson, I.I. Bigi, N. Uraltsev, *On the photon energy moments and their 'bias' corrections in $B \rightarrow X_s \gamma$* *Nucl. Phys. B* **710** (2005) 371 [hep-ph/0410080]
- [13] B. O. Lange, M. Neubert, G. Paz, *Theory of Charmless Inclusive B Decays and the Extraction of V_{ub}* *Phys. Rev. D* **72** (2005) 073006 [hep-ph/0504071]
- [14] T. Saito *et al.* [Belle Collaboration], *Measurement of the $\bar{B} \rightarrow X_s \gamma$ branching fraction with a sum of exclusive decays*, *Phys. Rev. D* **91** (2015) 052004
- [15] L. Pesantez *et al.* [Belle Collaboration], *Measurement of the Direct CP Asymmetry in $\bar{B} \rightarrow X_{s+d} \gamma$ Decays with a Lepton Tag*, *Phys. Rev. Lett.* **114** (2015) 151601
- [16] Belle Collaboration, *Measurement of the inclusive $B \rightarrow X_{s+d} \gamma$ branching fraction, photon energy spectrum and HQE parameters*, [arXiv:1608.02344]
- [17] Z. King *et al.* [Belle Collaboration], *Search for the decay $B^0 \rightarrow \phi \gamma$* , *Phys. Rev. D* **93** (2016) 111101
- [18] D. Dutta *et al.* [Belle Collaboration], *Search for $B_s^0 \rightarrow \gamma \gamma$ and a measurement of the branching fraction for $B_s^0 \rightarrow \phi \gamma$* , *Phys. Rev. D* **91** (2015) 011101 [arXiv:1411.7771]